Plant, Cell & Environment

WILEY

Plant, Cell & Environment

ORIGINAL ARTICLE

Warming and UV Radiation Alleviate the Effect of Virus Infection on the Microalga *Emiliania huxleyi*

Qianqian Fu[1,2] | Ruiping Huang[1,3] | Futian Li[4] | John Beardall[1,5,6] | David A. Hutchins[7] | Jingwen Liu[8] | Kunshan Gao[1,4]

[1]State Key Laboratory of Marine Environmental Science, College of Ocean and Earth Sciences, Xiamen University, Xiamen, China | [2]Yancheng Aquatic Science Research Institute, Yancheng Agricultural College, Yancheng, China | [3]State Key Laboratory of Marine Resources Utilization in South China Sea, Hainan University, Haikou, China | [4]Co-Innovation Center of Jiangsu Marine Bio-industry Technology, Jiangsu Ocean University, Lianyungang, China | [5]School of Biological Sciences, Monash University, Clayton, Victoria, Australia | [6]Faculty of Applied Sciences, UCSI University, Kuala Lumpur, Malaysia | [7]Marine and Environmental Biology, University of Southern California, Los Angeles, California, USA | [8]College of Ocean Food and Biological Engineering, Jimei University, Xiamen, China

Correspondence: Kunshan Gao (ksgao@xmu.edu.cn)

Received: 10 June 2024 | **Revised:** 15 October 2024 | **Accepted:** 22 October 2024

Funding: This study was supported by National Natural Science Foundation of China (42361144840) to KSG and by the US National Science Foundation grant OCE (1851222) to DAH.

Keywords: coccolithophore | *Emiliania huxleyi* | growth | ocean warming | photosynthesis | phytoplankton | UVR | virus

ABSTRACT

The marine microalga *Emiliania huxleyi* is widely distributed in the surface oceans and is prone to infection by coccolithoviruses that can terminate its blooms. However, little is known about how global change factors like solar UV radiation (UVR) and ocean warming affect the host-virus interaction. We grew the microalga at 2 temperature levels with or without the virus in the presence or absence of UVR and investigated the physiological and transcriptional responses. We showed that viral infection noticeably reduced photosynthesis and growth of the alga but was less harmful to its physiology under conditions where UVR influenced viral DNA expression. In the virus-infected cells, the combination of UVR and warming (+4°C) led to a 13-fold increase in photosynthetic carbon fixation rate, with warming alone contributing a change of about 5–7-fold. This was attributed to upregulated expression of genes related to carboxylation and light-harvesting proteins under the influence of UVR, and to warming-reduced infectivity. In the absence of UVR, viral infection downregulated the metabolic pathways of photosynthesis and fatty acid degradation. Our results suggest that solar UV exposure in a warming ocean can reduce the severity of viral attack on this ecologically important microalga, potentially prolonging its blooms.

1 | Introduction

The microalga *Emiliania huxleyi* is an important component of the marine phytoplankton, and is widespread within the upper mixed layer down 30 m (Nanninga and Tyrrell 1996). *E. huxleyi* forms blooms that can be terminated by coccolithoviruses (EhVs). EhVs are icosahedral double-stranded DNA-containing viruses belonging to the family Phycodnaviride (Castberg et al. 2002; Short et al. 2020). These viruses can routinely control or terminate phytoplankton blooms by lysing the host cells (Bratbak, Wilson, and Heldal Egge, and Heldal 1993, 1996; Knowles et al. 2020). This phenomenon has been suggested to be associated with virally induced disruption of photosynthesis (Kimmance et al. 2014). Viral infection has been shown to decrease the maximum photochemical efficiency of *E. huxleyi* (Kimmance et al. 2014; Bidle et al. 2007; Gilg et al. 2016), and a 20-fold increase in the concentration of a 2–200 nm size fraction containing viruses from seawater reduced primary production by about 50% (Gilg et al. 2016; Fuhrman 1999). Similarly, the red tide microalga *Phaeocystis globosa* showed decreased rates

of electron transport and net photosynthesis during viral infection (Chen, Gao, and Beardall 2015). Furthermore, marine viruses are suggested to influence biogeochemical cycles by lysing host cells (Fuhrman 1999; Wommack and Colwell 2000). Ocean climate change will impose direct and indirect effects on marine phytoplankton and viruses and their interactions (Chen, Gao, and Beardall 2015), thereby affecting marine ecosystems (Genner et al. 2004).

Since the mid-20th century, the anthropogenic emission of greenhouse gases has led to long-term warming over virtually the entire globe, and the world's oceans have absorbed over 90% of this excess heat (Gattuso et al. 2015). As a result, the ocean surface temperature is projected to rise by 2.6°C–4.8°C by the year 2100 (Gattuso et al. 2015). The projected extreme temperature increases of 3°C or more may result in the loss of some of these bloom-forming coccolithophore species from lower latitudes (Anderson et al. 2021; Hutchins and Tagliabue 2024). One consequence of this warming is enhanced stratification and shoaling of the upper mixed layer (Li et al. 2020), which can have both benefits and costs to photosynthetic organisms due to increased exposure to both visible and UV wavelengths of solar radiation (Gao et al. 2019). For instance, increased exposure to UV radiation (UVR) significantly decreases the rates of photosynthesis and calcification rate of *E. huxleyi* (Guan and Gao 2010), while warming can increase metabolic activities and may mitigate UV-induced damage by enhancing repairing mechanisms in phytoplankton cells (Gao, Zhang, and Häder 2018).

UVR reaching the Earth's surface is comprised of UVB (280–315 nm) and UVA (315–400 nm), with the latter reaching the Earth's surface almost quantitatively proportional to PAR (Häder and Gao 2023). UVR in surface oceans is probably among the most important abiotic stressors for phytoplankton and viruses as the algal host relies on light for energy, and viral survival is reduced under the influence of UVR (Horas, Theodosiou, and Becks 2018). Excessive UVR damages proteins, lipids, biomembranes, and other cellular organelles (Häder and Gao 2023). One of the main targets of UVR is DNA, with the most common damage being the formation of cyclobutane pyrimidine dimers (CPD) (Roeber et al. 2021). Phytoplankton cells have the capability to repair these lesions using the enzyme photolyase, which employs the energy of UVA and blue light to separate the dimers (Guan and Gao 2010). While UVR can induce DNA damage in both phytoplankton and viruses, DNA viruses containing thymine are commonly more sensitive to UV than RNA ones lacking thymine (Wilhelm et al. 2003; Mojica and Brussaard 2014). The sensitivity of different microalgal viruses to UVR varies due to differences in the ability of viruses to repair the damage caused by UVR (Mojica and Brussaard 2014). For instance, studies have shown that the virus EhV infecting *E. huxleyi* appears more susceptible to UVB than MpV, which infects *Micromonas pusilla* (Wilhelm et al. 2003; Jacquet et al. 2002; Jacquet and Bratbak 2003).

Temperature changes can influence viral infection by regulating virus abundance and infectivity. Most marine viruses can tolerate low temperatures, whereas increased temperatures reduce their infectivity and eventually cause inactivation (Nagasaki and Yamaguchi 1998; Martínez Martínez et al. 2015; Demory et al. 2017). Viral infection dynamics experiments have shown that warming above the optimal temperature for microalgal growth (T_{opt}) did not usually result in cell lysis and, notably, that temperatures below T_{opt} appeared to lengthen lytic cycle kinetics and reduce viral yield (Demory et al. 2017). The effect of temperature also depends on the locations from where the viruses were isolated. Although the viral production rate usually decreases with increasing temperature in temperate waters, the opposite trend occurs in polar-waters (Danovaro et al. 2011). Temperature also strongly affects virus-host interactions, but each virus-host system shows distinct responses (Horas, Theodosiou, and Becks 2018). For instance, an increase of 3°C reduced the abundance of the *E. huxleyi* virus EhV (Kendrick et al. 2014), although warming appeared to enhance virus population dynamics in a temperate plankton community (Frenken et al. 2020).

In contrast to temperature, little has been documented on the impacts of UVR on phytoplankton viruses and their interaction with hosts (Jacquet and Bratbak 2003; Kendrick et al. 2014). To the best of our knowledge, there have been no published reports on the combined effects of temperature and UVR on the microalgal host-virus relationship. Since temperature changes affect repair processes in phytoplankton cells by influencing the activity of the involved enzymes involved, we hypothesize that UVR may modulate the impacts of warming on the interaction between EhV and its host *E. huxleyi*. This is because UVR harms both the alga and its virus, while warming can stimulate repair processes in the host and reduce viral infectivity (Mojica and Brussaard 2014; Kendrick et al. 2014). We explored the combined effects of warming and UVR on the virus and its host and found that warming and UVR alleviated the negative effects of viral attack on *E. huxleyi* by regulating gene expression and enhancing photosynthetic performance in the virus-infected cells.

2 | Materials and Methods

2.1 | Material and Preculture Conditions

The coccolithophore *E. huxleyi* BOF92 and its virus EhV virus (EhV99B1) were isolated from the west coast of Norway (60°24′ N, 5°19′ E), where surface seawater temperatures can reach up to 18°C (Emery and Meincke 1986). The fresh EhV99B1 lysate for the infection experiment was prepared by infecting the host *E. huxleyi* and filtering the resulting lysate (0.22 μm PC membrane, Millipore, USA). The freshly harvested virus lysate was stored at 4°C for about 7 days in the dark for the subsequent infection experiments. For infection experiments, ~5 mL of this active viral lysate ($5–6 \times 10^8$ particles mL^{-1}) was added to an exponentially growing *E. huxleyi* culture ($5–6 \times 10^5$ cells mL^{-1}) in a 500 mL polycarbonate (PC) bottle (Castberg et al. 2002; Knowles et al. 2020).

The *E. huxleyi* cells were cultured in triplicate in 0.22 μm filtered natural seawater enriched with IMR/5 nutrients ($NO_3^- = 49.4$ μM, $PO_4^- = 5$ μM) and vitamins (Eppley, Holmes, and Strickland 1967) and grown at 17°C (similar to the current in situ temperature of the isolation site) or 21°C (representing the warming projected for the end of the 21st century). We grew the

cultures indoors under a constant PAR level of 400 μmol m^{-2} s^{-1} with a 12–12 light-dark cycle for > 8 generations (Supporting Information S1: Figure S1A). The initial cell concentration was 100 cells mL^{-1}, and the maximum cell concentration was controlled at less than 3–4 × 10^4 cells mL^{-1} by diluting the cultures every 7 days.

2.2 | Virus-Infection Experiment

Following the indoor culture, the *E. huxleyi* cells were transferred and grown at 17°C and 21°C outdoors (Supporting Information S1: Figure S1B,C), where they were initially exposed to fluctuating solar radiation without UVR (growth in 1 L PC bottles, opaque to UVR). The cultures (four replicates at each temperature treatment) were placed into two water tanks with the temperature controlled by a cooling unit (KW-010LR, China). The cultures were first exposed to about 55% natural solar radiation by covering them with a layer of neutral density screen for about 5 days, then removing the screen (100% incident solar radiation) for another 4 days with an average daytime PAR of about 500 μmol $m^{-2}s^{-1}$. Thereafter, the *E. huxleyi* cells were placed into and maintained in 500 mL quartz tubes (UV transparent) with an initial cell density of about 5 × 10^5 per mL, and about 5 mL of fresh EhV lysate was added to each of the exponentially growing cultures to make the ratio of virus to host cells about 10. Noninfected (control) treatments received the same volume of the sterilized medium. Subsequently, triplicate independent cultures of *E. huxleyi* were carried out with and without EhV under three solar radiation treatments: (1) P (PAR alone), using quartz tubes covered with 395 nm cut-off foil (Ultraphan UV Opak, Digefra), receiving irradiances above 395 nm; (2) PA (PAR + UVA), covered with 320 nm cut-off foil (Mntagefolie, Folex), receiving irradiance above 320 nm; (3) PAB (PAR + UVA + B), uncovered quartz tubes, receiving irradiances above 280 nm. The transmission spectra of the cut-off foils and the quartz have been presented previously (Zheng and Gao 2009). Incident solar radiation was continuously monitored by a broadband solar radiometer (ML-020P, EKO, Japan) that monitors PAR, UVA and UVB irradiances every second and records the means over each minute. The virus-host interaction experiments lasted for 4 days (Supporting Information S1: Figure S1D), during which time samples were taken at dawn, noon, and sunset for cell density measurements, virus production and effective photochemical efficiency (F_v'/F_m'). At midday of the third day (Supporting Information S1: Figure S1D), photosynthetic carbon fixation was determined, and the samples for Chl *a* content were collected and stored at −20°C before measurement. On the last day, the maximum quantum yield of PSII (F_v/F_m) was measured.

2.3 | Algal Cell and Virus Counts

The cell density and diameter of *E. huxleyi* were recorded directly by a Particle Counter and Size Analyzer (Z2, Beckman Coulter, USA). The specific growth rate (μ day^{-1}) was calculated using the following equation: $\mu\ (d^{-1}) = (\ln N_t - \ln N_{t\text{-}1})/\Delta t$, where N_t and $N_{t\text{-}1}$ are the cell numbers (cells mL^{-1}) over the time interval of Δt (t and $t-1$), respectively (Jiang et al. 2022). Culture samples of virus (2 mL) were collected and fixed with 40 μL 25% glutaraldehyde (0.5%, v/v, final concentration) for 15–30 min at 4°C in the dark before being frozen in liquid nitrogen and then stored at −80°C until analysis (Castberg et al. 2002; Brussaard et al. 2004). For analysis, the samples were thawed at room temperature and diluted in Tris-EDTA buffer (pH 8) at a final concentration of 10^5–10^6 particles mL^{-1}. The diluted samples were enumerated by a flow cytometer (Flow Cytometer, Epics Altra II, Beckman Coulter, USA) after staining with SYBR Green I (Invitrogen, USA) for 10 min at 80°C (Brussaard et al. 2004). The virus flow profile was analyzed using FCS Express 7 software.

2.4 | Burst Size

In this study, we assessed the latent period of EhV to be about 12 and 24 h after the infection at 17°C and 21°C, respectively. The viral burst size, the number of viruses produced during host cell lysis (Parada, Herndl, and Weinbauer 2006), was estimated as follows (Chen, Gao, and Beardall 2015):

Burst size = (maximum-minimum viral abundance)/numbers of lysed cells.

The number of lysed host cells was estimated by the maximum number minus the minimum number of the host cells. We calculated the burst size over the period 0–60 h after the infection when the number of EhV particles increased almost linearly (Figure 1).

2.5 | Assessment of Chlorophyll *a* Concentration and Fluorescence

Samples (30 mL) of cultures were filtered onto GF/F filters (25 mm, Whatman, USA) and extracted in 5 mL pure methanol at 4°C in darkness overnight. After the samples were centrifuged at 6000 g for 10 min (Universal 320 R, Hettich, Germany), the absorption values of the supernatant were measured at 632, 665, and 750 nm using an ultraviolet spectrophotometer (Tu-1810, Persee, China). The chlorophyll *a* concentration was calculated by the following equation (Ritchie 2006): Chl *a* (μg mL^{-1}) = 13.2654 × ($A_{665} - A_{750}$) − 2.6839 × ($A_{632} - A_{750}$). The maximum photochemical efficiency (F_v/F_m) of *E. huxleyi* was determined after 15 min dark adaption using a pulse-amplitude-modulated (PAM) fluorometer (Multi-colour-PAM-100, Walz, Effeltrich, Germany). The saturation pulse was 4000 μmol m^{-2} s^{-1} lasting 0.8 s. The maximum quantum yield of PSII (F_v/F_m) was described as $F_v/F_m = (F_m - F_0)/F_m$ (Kitajima and Butler 1975), where F_o and F_m represent the minimal fluorescence and the potential maximum fluorescence, respectively.

2.6 | Determination of Photosynthetic Carbon Fixation

In the middle of the photoperiod of the third day (Supporting Information S1: Figure S1D), triplicate borosilicate bottles (50 mL, one for a blank incubated in darkness) with the cells

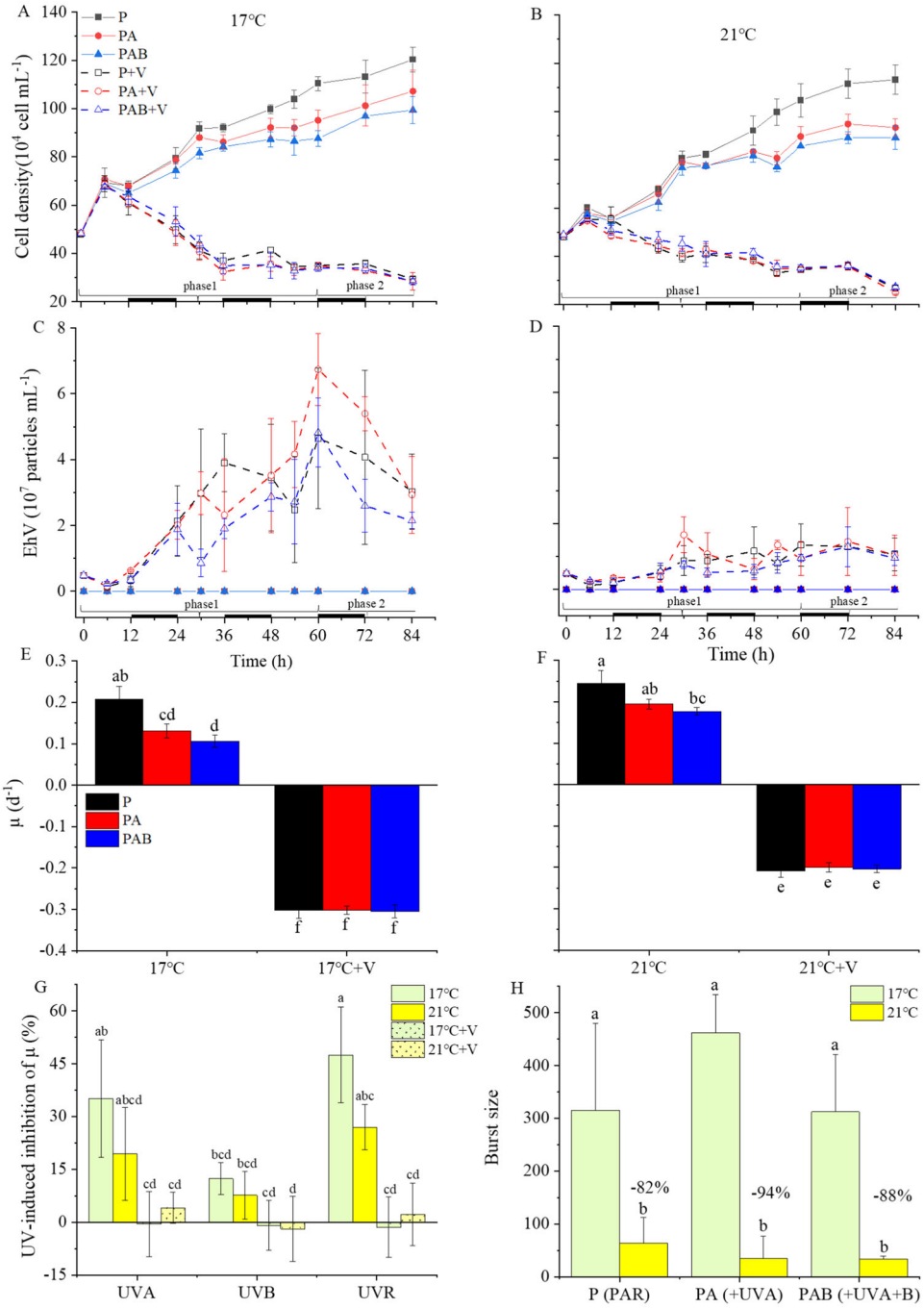

FIGURE 1 | Effects of UV irradiance and temperature on the interaction of the microalga *Emiliania huxleyi* and its virus EhV. Changes in the cell density of *E. huxleyi* over time at 17°C (A) and 21°C (B). Changes in the concentration of EhV particles during incubation at 17°C (C) and 21°C (D). The specific growth rates of *E. huxleyi* with (+V) or without (−V) the virus infections from 6 to 60 h at 17°C (E) and 21°C (F). The UV-induced inhibition of specific growth rates of *E. huxleyi* cells infected with (+V) or without (−V) EhV grown at 17°C and 21°C (G). The burst size of EhV at 17°C and 21°C (H) (0–60 h). The solid lines with solid symbols indicate data for cells noninfected with EhV, and the dotted lines with open symbols refer to cells infected with EhV. P, PA and PAB represent PAR alone, PAR + UVA and PAR + UVA + B, respectively. Phase 1 refers to the period of 0–60 h, and phase 2 to that from 60 to 84 h. Different letters above the bars represent statistically significant differences between the treatments in (E) and (F), letters apply to the data across both temperatures. The thick black lines on the abscissa in panels (A)–(D) show the dark periods. The data represent the means ± SD of triplicate cultures ($n = 3$). [Color figure can be viewed at wileyonlinelibrary.com]

from each culture were inoculated with 100 μL of 5 μCi (0.185 MBq) labelled $NaH^{14}CO_3$ solution (Amersham) and incubated for 3 h (noon period, solar light) with the mean PAR level of about 980 μmol m^{-2} s^{-1} before the samples were harvested onto Whatman GF/F filters. The filters were placed in 20 mL scintillation vial and fumed with HCl for 12 h before drying overnight at 60°C to remove residual inorganic carbon. Then, 5 mL of scintillation cocktail (Perkin Elmer) was added to the vials before counting with a liquid scintillation counter (Tri-Carb 2800 TR, Perkin-Elmer, USA). The photosynthetic carbon

fixation rate was calculated using the DIC values as described in a previous study (Supporting Information S1: Table S1) (Gao et al. 2007).

2.7 | Estimation of UV-Induced Inhibition

The inhibition by UVA, UVR and UVB of growth and photosynthesis rates was calculated as follows:

$$\mathrm{Inh}_{\mathrm{UVA}} = (RP - RPA)/(RP) \times 100\%$$

$$\mathrm{Inh}_{\mathrm{UVR}} = (RP - RPAB)/(RP) \times 100\%$$

$\mathrm{Inh}_{\mathrm{UVB}} = (RPA - RPAB)/(RP) \times 100\% = \mathrm{Inh}_{\mathrm{UVR}} - \mathrm{Inh}_{\mathrm{UVA}}$, where RP, RPA and RPAB represent the rates under P (PAR alone), PA (PAR + UVA) and PAB (PAR + UVA + B) treatments, respectively.

2.8 | Sample Collection, RNA Extraction, and Sequencing

Considering the greater abundance of virus at the low temperatures in contrast to 21°C, and that the physiology showed the same trend at both temperatures, we selected the 17°C treatment for transcriptome analyses. Since the PA (PAR + UVA) treatment showed a similar impact on the physiology of the microalgal cells as the PAB (PAR + UVA + B), we selected the P and PAB treatments for analysis. At the end of the infection experiment, we collected triplicate samples from the treatments with or without UVR for RNA extraction. Approximately 2×10^8 cells of each sample were collected and immediately stored at −80°C. Total RNA was extracted using a Trizol reagent kit (Invitrogen, Carlsbad, USA) according to the manufacturer's protocol. The extracted RNAs were used for sequencing with Illumina HiSeqTM 4000 by Gene Denovo Biotechnology Co., Ltd (Guangzhou, China).

2.9 | Bioinformatic Analysis

The raw reads were filtered using fastp (version 0.18.0) (Chen et al. 2018) by removing reads containing adapters, unknown nucleotides (N) (more than 10%) and low-quality reads [more than 50% of low-quality (Q-value ≤ 20) bases]. The clean reads were mapped to the reference genome (www.ncbi.nlm.nih.gov/genome/2?genome_assembly_id=22489) of *E. huxleyi* BOF92 using HISAT2 (version 0.18.0) (Kim, Langmead, and Salzberg 2015), and the FPKM (Reads Per Kilobase Million Mapped Reads) were calculated using RSEM (Li and Dewey 2011). Differentially expressed genes (DEGs) were identified using edgeR (3.12.1) based on the following criteria: fold change (FC) ≥ 1.5 and p-value < 0.05 (Fuertes et al. 2019). To assess the potential influences of UVR on the metabolism of *E. huxleyi*, KEGG pathway enrichment of DEGs was analyzed using a hypergeometric test with p-value < 0.05.

2.10 | Statistical Analysis

All physiological data were analyzed with SPSS software, using one-way ANOVA with post hoc investigation of the Tukey test after checking for homoscedasticity and additional normality (Shapiro–Wilk). The statistical methods were applied to the data across both temperatures. A $p < 0.05$ was used to indicate statistical significance. All values are represented as the means ± SD of triplicate cultures.

3 | Results

3.1 | Growth of the Algae

The changes in the microalgal cell density and the viral abundance showed the progressive nature of the viral infection (Figure 1). The numbers of *E. huxleyi* cells cocultured with EhV decreased significantly with a rapid increase of virus production in the cultures at 17°C and 21°C after 6 h (Figure 1A–D), and the viral infection resulted in negative growth after about 6 h following the infection (Figure 1E,F). As a consequence, the specific growth rate of the cells infected with the virus decreased significantly by about 246% ($p < 0.001$), 332% ($p < 0.001$), and 390% ($p < 0.001$) under PAR, PAR + UVA and PAR + UVA + B (P, PA and PAB treatments) at 17°C, respectively (Figure 1E), and by about 187% ($p < 0.001$), 203% ($p < 0.001$), and 215% ($p < 0.001$) at 21°C, corresponding, compared to that of noninfected cells (Figure 1F). UVR decreased the growth rate of *E. huxleyi* in the absence of the virus, but it did not result in significant growth changes in the presence of the virus (Figure 1E,F). UVR induced-inhibition of the algal growth in the absence of the viral infection was about 47.5%, more than the individual inhibitions brought about by UVA and UVB, which significantly decreased the growth by about 35.2% ($p < 0.001$) and 12.3% ($p < 0.001$) at 17°C, respectively (Figure 1G). At 21°C, UVR inhibited the growth rate by 27% ($p = 0.005$), with UVA and UVB contributing 19% and 8%, respectively (Figure 1G). The UVR-induced inhibition of growth with the viral infection was negative (−1.4%) and nearly nondetectable at 17°C, and was positive but less than 5% at 21°C (Figure 1G). In the *E. huxleyi* cultures without EhV, warming increased growth significantly by about 49% ($p = 0.009$) and 68% ($p = 0.003$) in the presence of UVA and UVA + B (PA and PAB), respectively (Figure 1E,F). In the presence of EhV, the warming treatment increased the growth rate of *E. huxleyi* by 30% ($p < 0.001$), 34% ($p < 0.001$) and 33% ($p < 0.001$) under PAR, +UVA and +UVA + B treatments (P, PA, PAB), respectively (Figure 1E,F). This indicates that the algal growth rate declined significantly less in the virus-infected cells under the influence of UVR at the warmer temperature.

3.2 | The Production of the Virus and its Burst Size

The virus production in the infected cultures of *E. huxleyi* was similar during the latent period (about 12 h), then rapidly increased at 17°C and slowly increased at 21°C in phase 1 (12–60 h). UVR reduced the production of the virus over the

infection period, although the difference was not significant at some time points. High temperature also decreased the virus production, as reflected in the concentration of viruses at 21°C and 17°C (Figure 1C,D). The presence of UVR appeared to decrease the release of viral particles, especially at 17°C. The burst size significantly decreased at 21°C compared to 17°C, by 82% ($p < 0.001$), 93% ($p < 0.001$), and 88% ($p < 0.001$) under P, PA, and PAB treatments, respectively (Figure 1H). At both temperatures, the presence of UVA or/and UVB did not cause significant changes in the burst size.

3.3 | Chl *a* Content

The viral infection significantly decreased Chl *a* content of *E. huxleyi* by about 83% ($p < 0.001$), 79% ($p < 0.001$), and 80% ($p < 0.001$) under the P, PA (PAR + UVA), and PAB (PAR + UVA + B) treatments at 17°C, respectively (Figure 2A), and by about 87% ($p < 0.001$), 87% ($p < 0.001$), and 77% ($p < 0.001$), respectively, at 21°C (Figure 2B).

The different radiation treatments had no significant effect on the Chl *a* content of the algal cells without the viral infection at both temperatures. In the cells infected with the virus, the Chl *a* content did not show significant change at 17°C, but increased at 21°C under the influence of UVR, by about 76% higher under PAR + UVA + B treatment compared with PAR + UVA ($p = 0.003$) (Figure 2A,B). No significant difference was found between the PAR and PAR + UVA treatments at 21°C ($p = 0.057$) (Figure 2B). A significant individual effect of temperature was observed on the *E. huxleyi* cells without the viral infection, but not in the culture with the virus. High temperature increased the Chl *a* content of *E. huxleyi* uninfected with the virus by 22% ($p < 0.001$), 12% ($p = 0.0317$), and 12% ($p < 0.001$) under P, PA and PAB treatments, respectively (Figure 2A,B). UVR and warming together increased the Chl *a* content of the cells infected with the virus by 71%, indicating an additive suppression of the viral attack on chlorophyll synthesis (Figure 2B).

3.4 | Photochemical Efficiency

The viral infection caused damage to the photosynthetic machinery of *E. huxleyi*, reducing the maximal photochemical efficiency (F_v/F_m) by about 52% ($p < 0.001$), 66% ($p < 0.001$), and 58% ($p < 0.001$) under PAR, PAR + UVA and PAR + UVA + B (P, PA and PAB) at 17°C, respectively, and by about 38% ($p < 0.001$), 32% ($p < 0.001$), and 25% ($p = 0.002$) respectively at 21°C, (Figure 2C,D). The F_v/F_m values of the virus-infected cells increased by about 49% ($p = 0.049$), 121% ($p < 0.001$) and 93% ($p < 0.001$) at 21°C compared to 17°C under the P, PA and PAB treatments, respectively (Figure 2C,D), indicating that warming moderated the virus- and UVR-induced damage to the algal photosystem II. The photosynthetic performance over time reflects the modulated infection process (Supporting Information S1: Figure S2). The viral infection similarly reduced the effective quantum yield; the presence of UVR reduced the yield in the cells not infected with virus but, in contrast, increased it in the cells infected with virus, again indicating a role of UVR-related suppression of viral attack. A comparison of the changing levels at the two temperature levels revealed that the warming alleviated the effects of the virus, either with or without UV (Supporting Information S1: Figure S2).

3.5 | Photosynthetic Carbon Fixation

Viral infection significantly decreased the photosynthetic carbon fixation per cell at 17°C and 21°C under all the solar radiation treatments with or without UVR (Figure 2E,F). At 17°C, the photosynthetic rate decreased by about 97% ($p < 0.001$), 96% ($p < 0.001$), and 95% ($p < 0.001$) under P, PA and PAB treatments, respectively (Figure 2E). At 21°C, it decreased respectively by 89% ($p < 0.001$) under PAR, by 85% ($p < 0.001$) under PAR + UVA, and by 72% ($p < 0.001$) under PAR + UVA + B (Figure 2F).

In the algal cells without the viral infection, the photosynthetic carbon fixation rate increased at 21°C compared to 17°C by 49% ($p < 0.001$) under PAR, by 61% ($p < 0.001$) under PAR + UVA and by 44% ($p < 0.001$) under PAR + UVA + B, indicating that the warming enhanced photosynthesis. In the virus-infected cultures at 21°C, the photosynthetic carbon fixation rate was still much lower compared to noninfected cells but was higher by about fivefold under PAR ($p = 0.033$), about sixfold ($p < 0.001$) under PAR + UVA, and about sevenfold ($p < 0.001$) under PAR + UVA + B, when compared to infected cultures at 17°C (Figure 2E,F). The photosynthetic carbon fixation based on Chl *a* showed the same trend at 17°C, in that the viral infection significantly reduced the rate. However, the virus infection did not significantly reduce the photosynthetic rate per Chl *a* at 21°C (Figure S3).

UV induced little inhibition of photosynthetic carbon fixation in *E. huxleyi* cells without the viral infection, and there was no significant difference between 17°C and 21°C. UVA and UVB reduced the effect of viral infection on the host's photosystem, with UVA contributing 17% and 35% and UVB contributing 63% and 104% at 17°C and 21°C, respectively. UV exposure relieved the viral infection by 80% and 139% at 17°C and 21°C, respectively, indicating that the warming treatment amplified the positive effect of UVR in the virus-infected cells (Figure 2G,H). In the virus-infected cells, the combination of UVR and warming brought about a 13-fold change in the carbon fixation rate compared to PAR alone treatment at 17°C. In parallel, the cellular particulate organic carbon (POC) increased significantly in the cultures with the virus at both temperatures and was higher at 21°C compared to 17°C in the virus-infected cells under UVR (Supporting Information S1: Figure S4).

3.6 | Transcriptomic Responses of the Alga to the Virus and UVR

The transcriptomic changes of the microalga in the presence of UVR or the virus reflect the impacts of UVR and virus on the molecular pathways (Figures 3 and 4). The abbreviations for enzymes involved in the metabolic pathways are shown in Supporting Information S1: Table S2. In the absence of UVR,

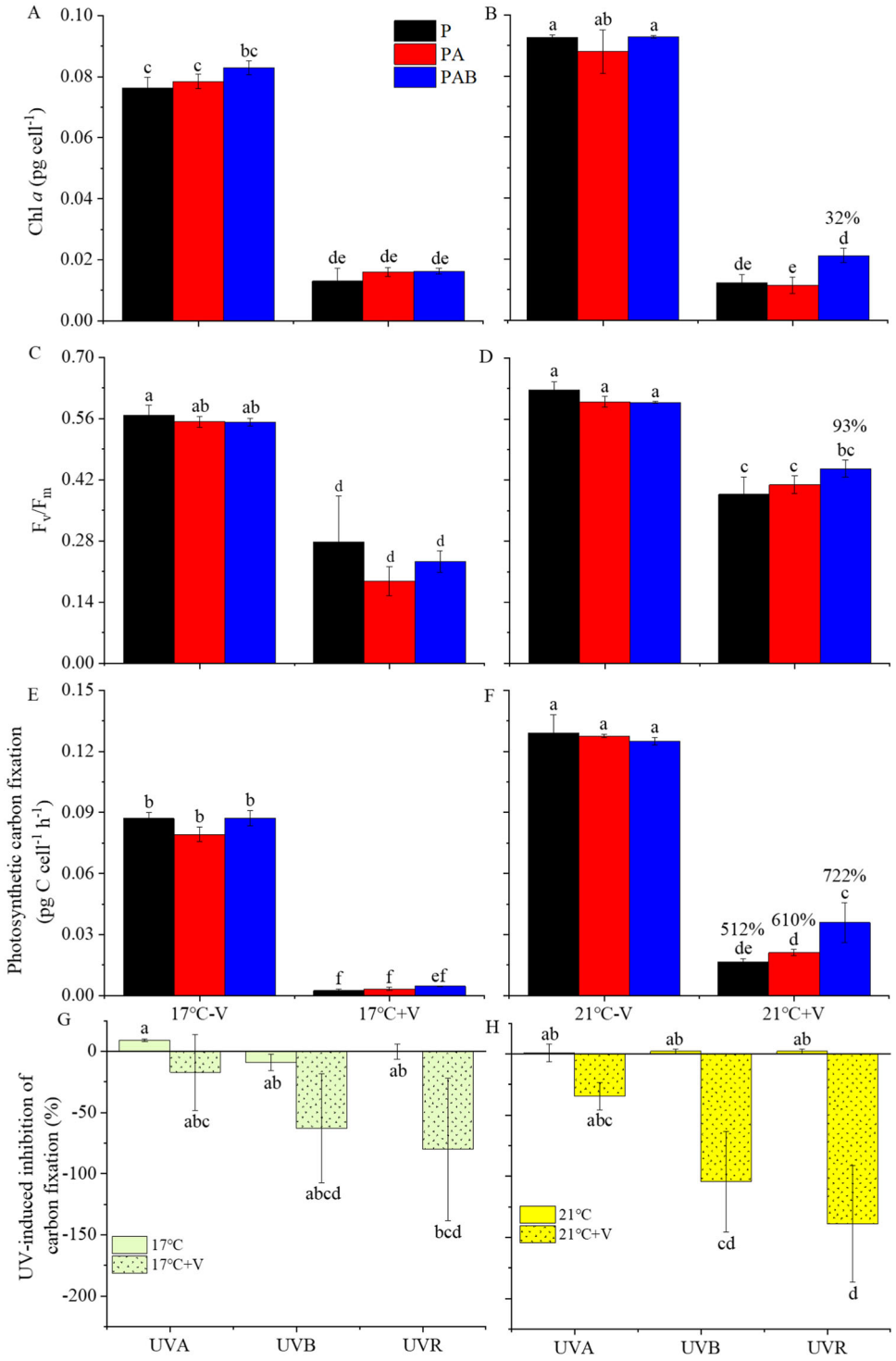

FIGURE 2 | Effects of UV irradiance and the virus EhV on Chl *a* and photosynthetic performances in *E. huxleyi* at two temperatures. The cellular concentration of Chl *a* at 17°C (A) and 21°C (B). The values of F_v/F_m at 17°C (C) and 21°C (D). The photosynthetic fixation carbon rate per cell at 17°C (E) and 21°C (F). The percentages above the column show changes induced by the warming. The UV-induced inhibition of photosynthetic carbon fixation per cell of *E. huxleyi* cells with (+V) or without (−V) virus EhV infection at 17°C (G) and 21°C (H). Symbols and abbreviations are the same as in Figure 1. The timings for the measurements are shown in Supporting Information S1: Figure S1. Different letters above the bars represent statistically significant differences between the treatments. In (A and B), (C and D), (E and F) and (G and H), letters apply to the data across both temperatures. The values represent means ± SD of triplicate cultures. [Color figure can be viewed at wileyonlinelibrary.com]

there were 2816 (6.17%) upregulated and 3717 (8.14%) downregulated genes in the virus-infected *E. huxleyi* cells (Supporting Information S1: Figure S5). The differentially expressed genes (DEGs) of *E. huxleyi* cells with and without the viral infection were significantly enriched in the pathways belonging nitrogen metabolism and photosynthesis-antenna proteins (Supporting Information S1: Figure S6A). In the pathway of nitrogen metabolism, except for genes encoding nitrate reductase (*NR*),

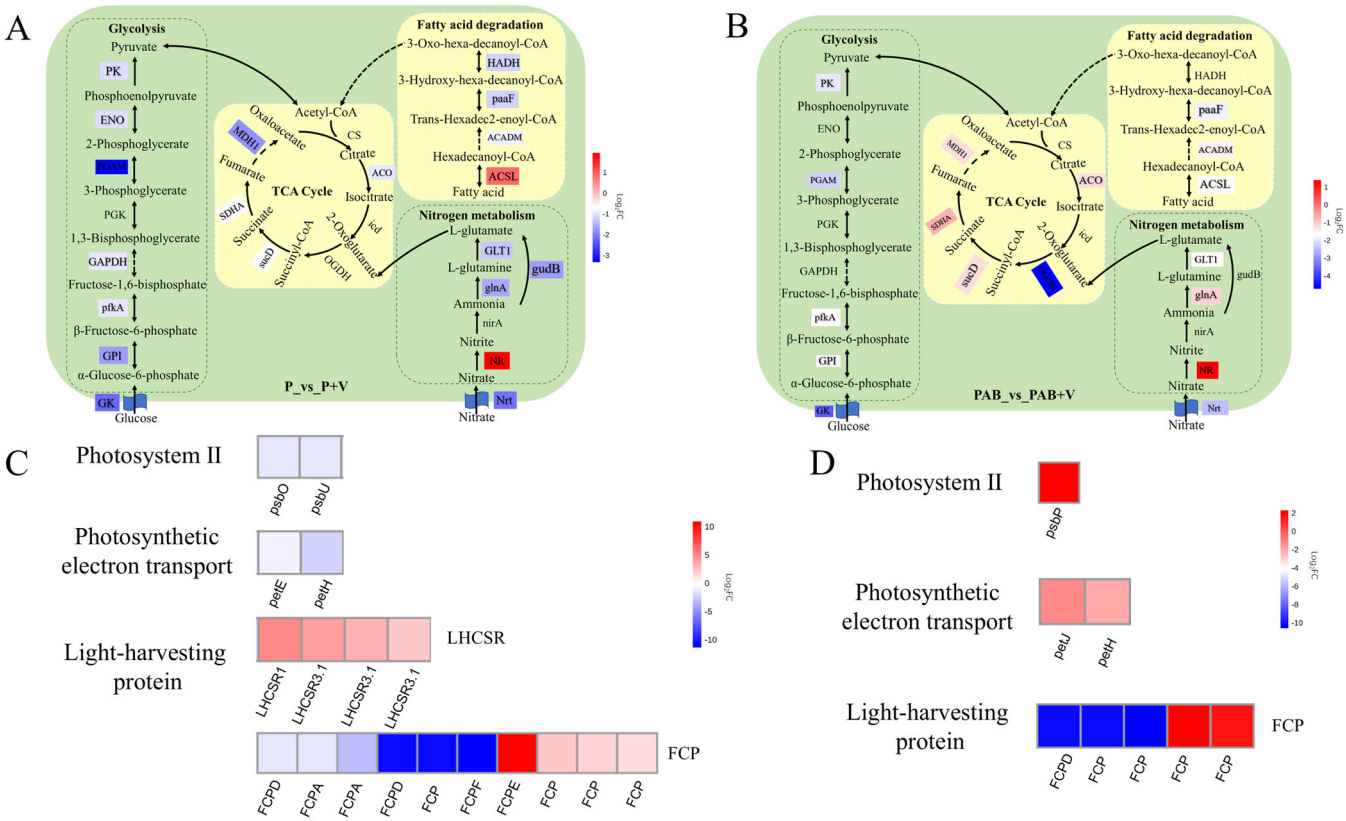

FIGURE 3 | The regulated pathways based on the differentially expressed genes (DEGs) between *E. huxleyi* cells with (+V) and without (−V) virus EhV infection under PAR (P) and PAR + UVR (PAB) at 17°C. Changes in expression of genes associated with different metabolic pathways in *E. huxleyi* infected with virus EhV under P (A) and PAB (B) treatment. Heatmap of genes related to photosynthesis of *E. huxleyi* infected with virus under P (C) and PAB (D) treatments. The red and blue colours, respectively, represent upregulation and downregulation. The colour scales represent the difference in $\log_2$FC. [Color figure can be viewed at wileyonlinelibrary.com]

the transcriptional levels of other genes (*NRT*, *nirA*, *glnA*, *gdhB* and *GLT1*) related to nitrogen uptake and assimilation were downregulated by the viral infection (Figure 3A). In terms of photosynthesis-antenna proteins, viral infection significantly influenced the transcriptional levels of genes encoding light-harvesting complex I chlorophyll-binding protein (*LHCSRs* and *FCPs*), with upregulation of eight genes (*FCPD* [two genes], FCPA [two genes], *FCP* [two genes], *FCPF*) and downregulation of six genes (*LHCSR1*, *LHCSR3.1* [three genes], *FCPE*, *FCP*) (Figure 3C). The transcriptional levels of genes related to other critical energy-related metabolism pathways, as reflected in those involved in fatty acid degradation (*paaF, ACADM*, and *HADH*), glycolysis (*GK*, *GPI*, *pfkA*, *GAPDH*, *PGAM*, *ENO*, and *PK*), the tricarboxylic acid cycle (TCA) (*ACO*, *sucD*, *SDHA* and *MDH1*) and photosynthesis-light reactions (*psbO*, *psbU*, *petE* and *petH*) were significantly downregulated with $\log_2$FC values ($\log_2$ scale of RPKM ratio between two samples) of 0.7–3.3 when the algal cells were infected by the virus (Figure 3A). Virus infection also downregulated the transcriptional levels of genes associated with DNA replication.

The number of DEGs induced by the viral infection was reduced by about 44.67%, when the cultures were exposed to UVR (PAR vs. PAB) (Figure 3B,D). The outcome of the KEGG pathway enrichment analysis suggested that viral infection under the influence of UVR significantly downregulated the transcriptional levels of genes associated with genetic information processing, including DNA replication, mismatch repair, nucleotide excision repair, base excision repair and proteasome (Supporting Information S1: Figure S6B). This indicates that DNA replication and repair were suppressed by the virus, and this effect was larger when cultures were exposed to UVR compared with PAR only. Viral infection also significantly influenced the transcriptional levels of genes related to the TCA cycle and nitrogen metabolism pathways, with the transcriptional levels of genes related to the TCA cycle (*ACO*, *OGDH*, *sucD*, *SDHA* and *MDH1*) and nitrogen metabolism (*GLT1*, *glnA* and *Nrt)* significantly downregulated for 0.8–4.7 $\log_2$FC (Figure 3B). The viral infection in the presence of UVR also significantly downregulated, for 1.5–3.6 $\log_2$FC, the transcriptional levels of genes related to glycolysis (*GK*, *GPI*, *pfkA*, *PGAM* and *PK*) and fatty acid degradation (*ACSL, ACADM* and *paaF*), although DEGs were not significantly enriched in glycolysis or fatty acid degradation (Figure 3B). When the cells were exposed to UVR, the viral infection also influenced transcriptional levels of genes related to Photosystem II (*PsbP*), photosynthetic electron transport (*petJ* and *petH*) and photosynthesis light-harvesting proteins (*FCPs*), but to a lesser extent compared to the PAR alone treatment (Figure 3D), indicating a suppressive impact of UVR on the viral attack in terms of transcriptomic responses.

For *E. huxleyi* cells free of the virus, the PAB (PAR + UVR) group had 4338 (9.51%) upregulated and 2274 (4.98%) downregulated genes (Supporting Information S1: Figure S5) compared with cells exposed to PAR alone. The DEGs associated with the pathway of

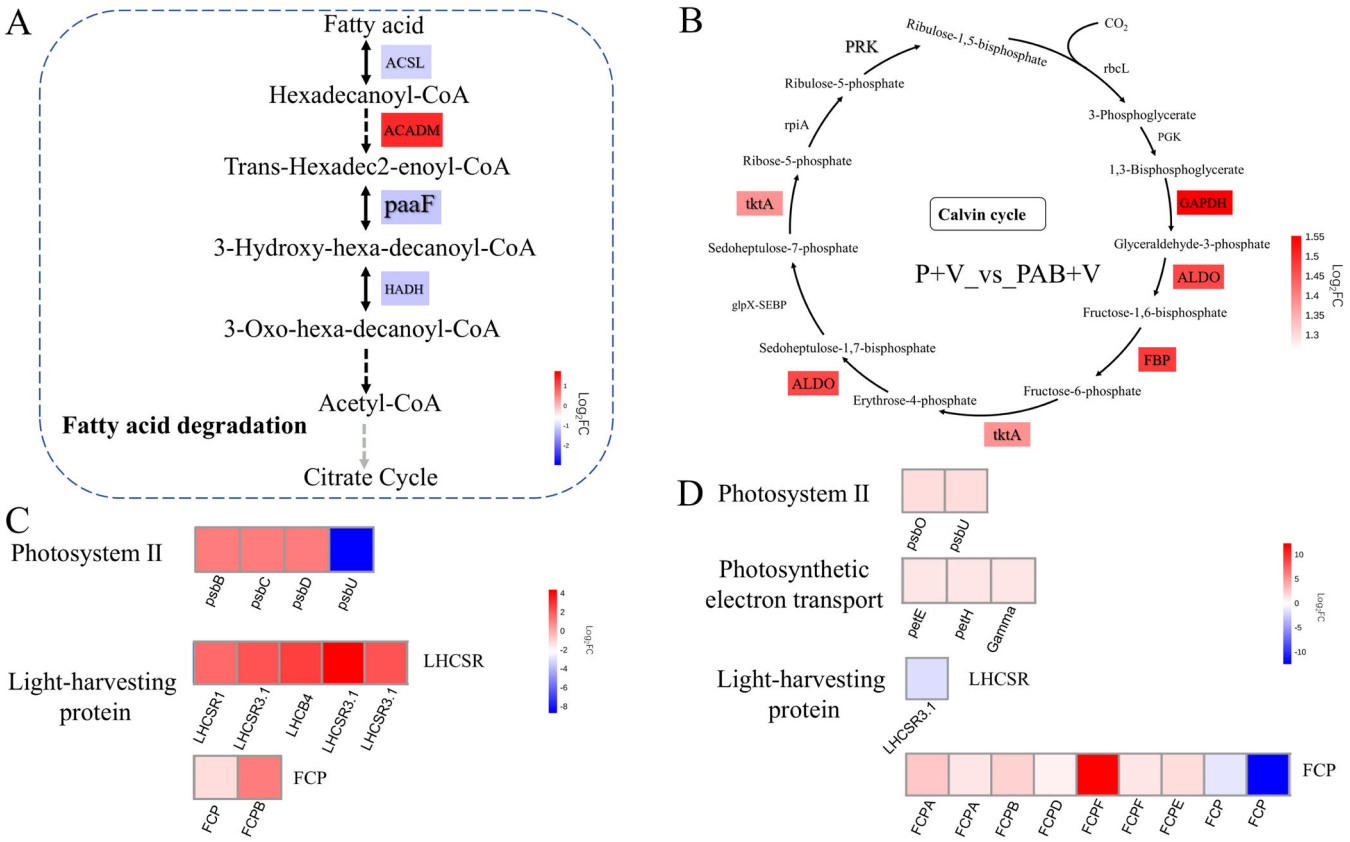

FIGURE 4 | The regulated pathways based on the differentially expressed genes (DEGs) between P (PAR alone) and PAB (PAR + UVR) treatment in *E. huxleyi* with (+V) and without (−V) EhV infection at 17°C. Changes in expression of genes associated with fatty acid degradation pathway without virus infection (−V) but with UVR (A). Changes in expression of genes associated with Calvin cycle pathway of the cells with the virus infection and UVR (B). Heatmap of genes related to photosynthesis while *E. huxleyi* noninfected (C) and infected (D) with the virus. The red and blue colours respectively represent upregulation and downregulation. The colour scales represent the difference in $\log_2$FC. [Color figure can be viewed at wileyonlinelibrary.com]

fatty acid degradation were enriched (Supporting Information S1: Figure S6C), and the transcriptional levels of genes related to *ACADM* were upregulated while *ACLD*, *paaF* and *HADH* were significantly downregulated for 1.0–1.1 $\log_2$FC under influence of UVR (Figure 4A). UVR significantly upregulated, for 1–4 $\log_2$FC, the transcriptional levels of the genes related to photosystem II (*psb* B, *psb* C and *psb* D) and photosynthesis harvesting proteins (*LHCSRs* and *FCPs*) (Figure 4C). In terms of genetic information processing, UVR upregulated genes associated with DNA replication, ribosome and ribosome biogenesis, mismatch repair, nucleotide excision repair and homologous recombination (Supporting Information S1: Figure S6C).

For *E. huxleyi* cells infected with the virus, UVR exposure resulted in 653 (1.43%) upregulated and 763 (1.67%) downregulated genes (Supporting Information S1: Figure S5). The pathway enrichment analysis showed that photosynthetic carbon fixation and light-harvesting antenna proteins were the most significantly enriched pathways under the influence of UVR (Supporting Information S1: Figure S6D). In the Calvin cycle, UVR significantly upregulated the transcriptional levels of genes related to *GAPDH*, *ALDO*, *FBP*, *tktA* and *PRK* for 1.1–1.6 $\log_2$FC (Figure 4B). In addition, UVR upregulated, for 1.0–12 $\log_2$FC, the transcriptional levels of genes related to photosystem II (*psbO*, *psbU*), photosynthetic electron transport (*petE* and *petF*), F-type ATPase (*gamma*), as well as photosynthesis harvesting proteins (*FCPs*) (Figure 4D). In addition, UVR upregulated the genes associated with genetic information processing DNA replication and ribosomes (Supporting Information S1: Figure S6D), with a smaller magnitude of changes when *E. huxylei* was infected by virus compared to the cells free of virus.

4 | Discussion

Our results indicate that viral attack on *E. huxleyi* by EhV was suppressed by warming and solar UVR. Although we did not measure the transcriptomes at 21°C, the physiological responses showed the same trends at both temperatures. In the algal cells infected with the virus, the photosynthetic carbon fixation rate was 13-fold higher under the UVR and warming treatments compared to 17°C cultures under PAR alone, with warming alone contributing about a five- to sevenfold change. While UVR harms both the host and the virus, reducing the growth rate of the alga and damaging the viral DNA, UVR's effect on the virus overrode its impact on the host. UVR thus suppressed viral harm to the pathways of photosynthesis, fatty acid degradation, TCA cycle and nitrogen metabolism, and led to UV-induced enhancement of photosynthetic carbon fixation of the host algal cells infected with the virus.

4.1 | The Harm Caused to the Host by the Virus

The viral infection reduced photosynthesis, as evidenced by chlorophyll content, photochemical quantum yield, and photosynthetic carbon fixation, as reported previously (Kimmance et al. 2014; Bidle et al. 2007; Gilg et al. 2016; Fu and Gao 2022), and so contributed to a decline in host growth. Viral infection can shut down host protein synthesis and decrease the supply of proteins D1 (*psbA*) and D2 (*psbD*) for the photosystem II core reaction center (Arias, Lenardon, and Taleisnik 2003; Lindell et al. 2004). This decreases the capacity for PSII repair and assembly, followed by an accumulation of damaged PSII complexes (Gilg et al. 2016). We did not verify directly that the viral infection downregulated the D1 and D2 proteins from our transcriptomic results; however, the transcriptional levels of genes related to the PSII peripheral protein and light-harvesting proteins *FCPs* were downregulated in the algal cells infected with the virus. In addition, the effects of virus infection are considered to be associated with virally induced interruption of electron transport between photosystems (Kimmance et al. 2014), which was also observed at transcriptional levels in the present study (Figure 3C,D). The downregulated transcription of genes related to photosystems and the photosynthetic electron chain could lead to the observed reduction in photochemical quantum yield. This supported the hypothesis that the virus-induced decreases in photosynthetic carbon fixation and thus growth were due to a decline in energy supply from the algal photosynthetic system (Sydney et al. 2014; Woodworth et al. 2015).

The viral infection also downregulated transcriptional levels of genes related to fatty acid degradation and nitrogen uptake and assimilation to glutamate in *E. huxleyi*. Viruses exhibit much higher N:C and P:C than their phytoplankton hosts (Jover et al. 2014). Previous studies have shown that the viral genome was being overproduced relative to capsids produced by the hosts when EhV infected *E. huxleyi* (Nissimov et al. 2016; Maat and Brussaard 2016), which implies that EhV needs large supplies of ammonia and lipids for packaging. In the present study, the transcriptional downregulation of genes involved in fatty acid degradation suggested that accumulated fatty acid may be used for the biosynthesis of viral lipid membranes (Chukkapalli, Heaton, and Randall 2012). It would have been logical to measure fatty acid content to supplement the data on gene expression, but sample limitations precluded this. In terms of viral nitrogen demand, the reduced nitrogen uptake and assimilation in *E. huxlyei* may be compensated by viral-induced ammonia uptake (Monier et al. 2017). Therefore, the reduction in energy production, as well as nitrogen uptake and assimilation contributed to the suppressed growth of *E. huxleyi* with viral infection. The downregulated transcription of genes related to glycolysis and the TCA cycles, which are energy production pathways, may also be responsible for the decline in growth of *E. huxlyei*.

4.2 | The Effects of UVR on the Host Alga and its Virus

UVR causes damage to DNA and PSII reaction centres in phytoplankton and increases the energy budget needed for PSII repair (Jiang et al. 2022; Xing, Gao, and Beardall 2015), which is consistent with the lower rates of growth and photosynthesis in *E. huxleyi* in the cultures exposed to UVR but free of the virus. The effect of UVB was almost overwhelmed by that of UVA (Figures 1G and 2G,H), probably because the incident intensity of UVA was about 40 times that of UVB, though the energy per quantum photon of the latter is greater than that of the former. UVR exposure led to distinct transcriptomic imprints, downregulating the energy metabolism pathway associated with fatty acid degradation. Therefore, it is probable that UVR damaged DNA and photosystems, and subsequently reduced energy supply by downregulating energy metabolism pathways, leading to the reduction in the growth rate (Figure 1A,B). However, the tradeoffs associated with viral infection of algae may have the potential to alter their responses to environmental factors. In our study, the *E. huxleyi* cells infected with the virus benefitted from UVR exposure, with increased levels of Chl *a*, quantum yield and photosynthetic carbon fixation (Figure 2B,D,E,F). Although the cell density and specific growth rate in the virus-infected algal cells did not exhibit significant changes among the radiation treatments, such physiological enhancement in the presence of UVR must be attributed to its suppression of viral attack, since the virus gene transcription was altered (Figure 5). The transcriptomics of the algal cells infected with the virus showed that the Calvin cycle was upregulated under the influence of UVR exposure, which explains why UVR stimulated the photosynthetic carbon fixation respectively by 80% at 17°C and by 139% at 21°C (Figure 2E,F).

It has been reported that about 30% of the viral mortality at the sea surface could be caused by UVR exposure (Yuan et al. 2011). Marine viruses are suggested to be more sensitive to UVR than microalgae, and exhibit virus-specific responses to UVR due to their genome characteristics, capsid structure and/or repair mechanisms (Jacquet and Bratbak 2003; Yuan et al. 2011; Kellogg and Paul 2002). UVR has been show to negatively impact the virus EhV for *E. huxleyi*, but not to affect the CeV virus for *Chrysochromulina ericina* and the PoV-virus for *Pyramimonas orientalis* (Jacquet and Bratbak 2003). In our study, UVR upregulated the folate biosynthesis pathway of EhV, affecting the production of dihydrofolic acid and regeneration of tetrahydrofolate by dihydrofolate reductase (coded by gene-*EhV113* in this study) via reductive methylation (Whitaker et al. 1995). Therefore, UVR exposure may lead to DNA methylation in viruses, but the specific mechanisms need to be explored.

4.3 | The Effects of Warming on Virus-Host Interactions

A previous study reported that rising temperature induced viral resistance in *E. huxleyi* as virus abundances were lower, and cell abundances and Fv/Fm of the host were higher in the treatment with higher temperature (+3°C) (Kendrick et al. 2014). In our study, we also observed that warming (+4°C) reduced the concentration of EhV particles, and increased the RGR, F_v/F_m and photosynthetic carbon fixation of *E. huxleyi* infected with virus (Figures 1D,E and 2D,F). This could potentially be due to warming-altered membrane-bound surface receptors reducing the infectivity of the virus EhV to *E. huxleyi*, leading to much fewer viral particles being released in the culture (Mojica and Brussaard 2014; Kendrick et al. 2014).

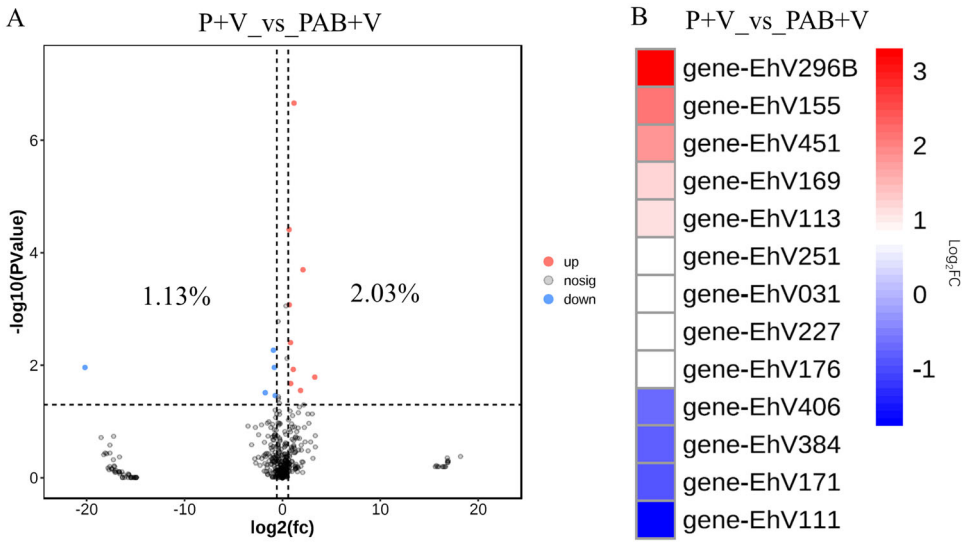

FIGURE 5 | Differentially expressed genes (DEGs) between the solar radiation treatments with (PAB) and without (P) UVR for the virus EhV (A). The heatmap of its relative gene expressions (B). [Color figure can be viewed at wileyonlinelibrary.com]

Temperature changes can influence the infectivity of virus and host-virus interactions (Horas, Theodosiou, and Becks 2018). It has been reported that PgVs-infecting *Phaeocystis globosa* were inactivated above 35°C, while infectivity of Group II PgVs could only be maintained below 25°C (Baudoux and Brussaard 2005), since thermal changes impact structure and elasticity of proteins and membrane lipids of virus (Mojica and Brussaard 2014). The effects of temperature on viruses will most likely arise from viral structural changes that regulate the sensitivity of viral lipid membranes or capsid proteins to thermal deformation or thermal fracture (Horas, Theodosiou, and Becks 2018; Selinger et al. 1991; Evilevitch et al. 2008). Temperature changes are known to affect the stability of viral capsid proteins, as well as the folding and binding of proteins and nucleic acids (Mojica and Brussaard 2014), and can therefore directly affect viral proliferation or indirectly affect the efficiency of viral infection of the host.

4.4 | Ecological Significance

Viruses are major contributors to marine phytoplankton mortality, diverting energy and biomass from higher trophic level herbivore-mediated food webs to microbially mediated pools of recyclable dissolved organic matter. This reduces the transfer of carbon or nutrients to higher trophic levels and enhances nutrient recycling by lysing cells (Mojica et al. 2016), thus, playing a key role in biogeochemical cycling (Mojica and Brussaard 2014; Zhang, Weinbauer, and Peduzzi 2021).

The microalga *E. huxleyi* is distributed in almost all ocean ecosystems from the equator to sub-polar regions, and occasionally forms blooms of up to 100 000 km^2. Its virus EhV is known to play an important role in terminating these blooms. The findings in the present work imply that warming and UVR can work together to alleviate the viral infection of *E. huxleyi*. Consequently, *E. huxleyi* blooms could be less harmed by the virus, leading to an extended bloom period of the alga under the influences of future warming and UVR. Virus infections in aquatic ecosystems lead to cell lysis, which converts POC into dissolved organic carbon (DOC) (Suttle 2005), altering the efficiency of the biological carbon pump (Brussaard et al. 2008). Viral infection of *E. huxleyi* might facilitate the downward vertical flux of POC (Laber et al. 2018), and we detected increased cellular POC in the virus-infected cells (Supporting Information S1: Figure S4), However, UVR and warming-related suppression of the virus EhV and the host-virus interaction is likely to differ in different regions or under different weather conditions, especially depending when and where the microalga is forming blooms. In view of ocean global changes, ocean warming is predicted to decrease the thickness of the upper mixed layer in subtropical regions, which increases exposure of the cells within these layers to UVR. Consequently, *E. huxleyi* blooms may be expected to last longer due to the antagonistic and/or synergistic effects of UVR and warming on the microalga, the virus and the host-virus interactions.

There has been limited research on the interactive effects of temperature and UVR on viral infection in microalgae. Our results are limited to one species at the levels of physiological and transcriptomic responses. Therefore, future work is needed to investigate in more detail how the current status of global climate warming under incident solar radiation in the presence of UVR impacts the survival of a broader range of marine microalgae under viral infection, thereby laying a theoretical foundation for explaining the exacerbation of algal blooms under ocean climate changes.

Acknowledgements

The authors are grateful to He Li for his technical assistance and to the laboratory engineers Xianglan Zeng and Wenyan Zhao for their logistical and technical support. This study was supported by National Natural Science Foundation of China (42361144840) to KSG and by the US National Science Foundation grant OCE (1851222) to DAH.

Conflicts of Interest

The authors declare no conflicts of interest.

Data Availability Statement

The data that support the findings of this study are available on request from the corresponding author. The data are not publicly available due to privacy or ethical restrictions.

References

Anderson, S. I., A. D. Barton, S. Clayton, S. Dutkiewicz, and T. A. Rynearson. 2021. "Marine Phytoplankton Functional Types Exhibit Diverse Responses to Thermal Change." *Nature Communications* 12: 6413.

Arias, M. C., S. Lenardon, and E. Taleisnik. 2003. "Carbon Metabolism Alterations in Sunflower Plants Infected With the *Sunflower Chlorotic Mottle Virus*." *Journal of Phytopathology* 151: 267–273.

Baudoux, A.-C., and C. P. D. Brussaard. 2005. "Characterization of Different Viruses Infecting the Marine Harmful Algal Bloom Species *Phaeocystis globosa*." *Virology* 341: 80–90.

Bidle, K. D., L. Haramaty, J. Barcelos e Ramos, and P. Falkowski. 2007. "Viral Activation and Recruitment of Metacaspases in the Unicellular Coccolithophore, *Emiliania huxleyi*." *Proceedings of the National Academy of Sciences* 104: 6049–6054.

Bratbak, G., J. Egge, and M. Heldal. 1993. "Viral Mortality of the Marine Alga *Emiliania huxleyi* (Haptophyceae) and Termination of Algal Blooms." *Marine Ecology Progress Series* 93: 39–48.

Bratbak, G., W. Wilson, and M. Heldal. 1996. "Viral Control of *Emiliania huxleyi* Blooms?" *Journal of Marine Systems* 9: 75–81.

Brussaard, C. P., S. W. Wilhelm, F. Thingstad, et al. 2008. "Global-Scale Processes With a Nanoscale Drive: The Role of Marine Viruses." *The ISME Journal* 2: 575–578.

Brussaard, C. P. D., S. M. Short, C. M. Frederickson, and C. A. Suttle. 2004. "Isolation and Phylogenetic Analysis of Novel Viruses Infecting the Phytoplankton *Phaeocystis globosa* (Prymnesiophyceae)." *Applied and Environmental Microbiology* 70: 3700–3705.

Castberg, T., R. Thyrhaug, A. Larsen, et al. 2002. "Isolation and Characterization of a Virus That Infectsemiliania Huxleyi(Haptophyta)1." *Journal of Phycology* 38: 767–774.

Chen, S., K. Gao, and J. Beardall. 2015. "Viral Attack Exacerbates the Susceptibility of a Bloom-Forming Alga to Ocean Acidification." *Global Change Biology* 21: 629–636.

Chen, S., Y. Zhou, Y. Chen, and J. Gu. 2018. "Fastp: An Ultra-Fast All-In-One FASTQ Preprocessor." *Bioinformatics* 34: i884–i890.

Chukkapalli, V., N. S. Heaton, and G. Randall. 2012. "Lipids at the Interface of Virus-Host Interactions." *Current Opinion in Microbiology* 15: 512–518.

Danovaro, R., C. Corinaldesi, A. Dell'Anno, et al. 2011. "Marine Viruses and Global Climate Change." *FEMS Microbiology Reviews* 35: 993–1034.

Demory, D., L. Arsenieff, N. Simon, et al. 2017. "Temperature Is a Key Factor in *Micromonas*-Virus Interactions." *ISME Journal* 11: 601–612.

Emery, W., and J. Meincke. 1986. "Global Water Masses-Summary and Review." *Acta Oceanl Sin* 9: 383–391.

Eppley, R. W., R. W. Holmes, and J. D. H. Strickland. 1967. "Sinking Rates of Marine Phytoplankton Measured With a Fluorometer." *Journal of Experimental Marine Biology and Ecology* 1: 191–208.

Evilevitch, A., L. T. Fang, A. M. Yoffe, et al. 2008. "Effects of Salt Concentrations and Bending Energy on the Extent of Ejection of Phage Genomes." *Biophysical Journal* 94: 1110–1120.

Frenken, T., C. P. D. Brussaard, M. Velthuis, et al. 2020. "Warming Advances Virus Population Dynamics in a Temperate Freshwater Plankton Community." *Limnology and Oceanography Letters* 5: 295–304.

Fu, Q., and K. Gao. 2022. "Reduced Salinity Exacerbates the Viral Infection on the Coccolithophorid *Emiliania huxleyi* at Elevated pCO_2." *Frontiers in Marine Science* 9: 1091476.

Fuertes, I., B. Campos, C. Rivetti, B. Piña, and C. Barata. 2019. "Effects of Single and Combined Low Concentrations of Neuroactive Drugs on *Daphnia magna* Reproduction and Transcriptomic Responses." *Environmental Science & Technology* 53: 11979–11987.

Fuhrman, J. A. 1999. "Marine Viruses and Their Biogeochemical and Ecological Effects." *Nature* 399: 541–548.

Gao, K., J. Beardall, D.-P. Häder, J. M. Hall-Spencer, G. Gao, and D. A. Hutchins. 2019. "Effects of Ocean Acidification on Marine Photosynthetic Organisms Under the Concurrent Influences of Warming, UV Radiation, and Deoxygenation." *Frontiers in Marine Science* 6: 322.

Gao, K., Y. Wu, G. Li, H. Wu, V. E. Villafañe, and E. W. Helbling. 2007. "Solar UV Radiation Drives Co_2 Fixation in Marine Phytoplankton: A Double-Edged Sword." *Plant Physiology* 144: 54–59.

Gao, K., Y. Zhang, and D.-P. Häder. 2018. "Individual and Interactive Effects of Ocean Acidification, Global Warming, and Uv Radiation on Phytoplankton." *Journal of Applied Phycology* 30: 743–759.

Gattuso, J.-P., A. Magnan, R. Billé, et al. 2015. "Contrasting Futures for Ocean and Society From Different Anthropogenic Co_2 Emissions Scenarios." *Science* 349: aac4722.

Genner, M. J., D. W. Sims, V. J. Wearmouth, et al. 2004. "Regional Climatic Warming Drives Long–Term Community Changes of British Marine Fish." *Proceedings of the Royal Society of London. Series B: Biological Sciences* 271: 655–661.

Gilg, I., S. Archer, S. Floge, et al. 2016. "Differential Gene Expression Is Tied to Photochemical Efficiency Reduction in Virally Infected *Emiliania huxleyi*." *Marine Ecology Progress Series* 555: 13–27.

Guan, W., and K. Gao. 2010. "Impacts of UV Radiation on Photosynthesis and Growth of the Coccolithophore *Emiliania huxleyi* (Haptophyceae)." *Environmental and Experimental Botany* 67: 502–508.

Häder, D.-P., and K. Gao. 2023. "Aquatic Productivity Under Multiple Stressors." *Water* 15: 817.

Horas, E. L., L. Theodosiou, and L. Becks. 2018. "Why Are Algal Viruses Not Always Successful?" *Viruses* 10: 474.

Hutchins, D. A., and A. Tagliabue. 2024. "Feedbacks Between Phytoplankton and Nutrient Cycles in a Warming Ocean." *Nature Geoscience* 17: 495–502.

Jacquet, S., and G. Bratbak. 2003. "Effects of Ultraviolet Radiation on Marine Virus-Phytoplankton Interactions." *FEMS Microbiology Ecology* 44: 279–289.

Jacquet, S., M. Heldal, D. Iglesias-Rodriguez, A. Larsen, W. Wilson, and G. Bratbak. 2002. "Flow Cytometric Analysis of an *Emiliana huxleyi* Bloom Terminated By Viral Infection." *Aquatic Microbial Ecology* 27: 111–124.

Jiang, X., Y. Zhang, D. A. Hutchins, and K. Gao. 2022. "Nitrogen-Limitation Exacerbates the Impact of Ultraviolet Radiation on the Coccolithophore *Gephyrocapsa oceanica*." *Journal of Photochemistry and Photobiology B: Biology* 226: 112368.

Jover, L. F., T. C. Effler, A. Buchan, S. W. Wilhelm, and J. S. Weitz. 2014. "The Elemental Composition of Virus Particles: Implications for Marine Biogeochemical Cycles." *Nature Reviews Microbiology* 12: 519–528.

Kellogg, C., and J. Paul. 2002. "Degree of Ultraviolet Radiation Damage and Repair Capabilities Are Related to G+C Content in Marine Vibriophages." *Aquatic Microbial Ecology* 27: 13–20.

Kendrick, B. J., G. R. DiTullio, T. J. Cyronak, J. M. Fulton, B. A. S. Van Mooy, and K. D. Bidle. 2014. "Temperature-Induced Viral Resistance in *Emiliania huxleyi* (Prymnesiophyceae)." *PLoS One* 9: e112134.

Kim, D., B. Langmead, and S. L. Salzberg. 2015. "HISAT: A Fast Spliced Aligner With Low Memory Requirements." *Nature Methods* 12: 357–360.

Kimmance, S., M. Allen, A. Pagarete, J. Martínez Martínez, and W. Wilson. 2014. "Reduction in Photosystem II Efficiency During a Virus-Controlled *Emiliania huxleyi* Bloom." *Marine Ecology Progress Series* 495: 65–76.

Kitajima, M., and W. L. Butler. 1975. "Quenching of Chlorophyll Fluorescence and Primary Photochemistry in Chloroplasts by Dibromothymoquinone." *Biochimica et Biophysica Acta (BBA)—Bioenergetics* 376: 105–115.

Knowles, B., J. A. Bonachela, M. J. Behrenfeld, et al. 2020. "Temperate Infection in a Virus–Host System Previously Known for Virulent Dynamics." *Nature Communications* 11: 4626.

Laber, C. P., J. E. Hunter, F. Carvalho, et al. 2018. "Coccolithovirus Facilitation of Carbon Export in the North Atlantic." *Nature Microbiology* 3: 537–547.

Li, B., and C. N. Dewey. 2011. "RSEM: Accurate Transcript Quantification from RNA-Seq Data With or Without a Reference Genome." *BMC Bioinformatics* 12: 323.

Li, G., L. Cheng, J. Zhu, K. E. Trenberth, M. E. Mann, and J. P. Abraham. 2020. "Increasing Ocean Stratification Over the Past Half-Century." *Nature Climate Change* 10: 1116–1123.

Lindell, D., M. B. Sullivan, Z. I. Johnson, A. C. Tolonen, F. Rohwer, and S. W. Chisholm. 2004. "Transfer of Photosynthesis Genes to and From *Prochlorococcus* Viruses." *Proceedings of the National Academy of Sciences* 101: 11013–11018.

Maat, D., and C. Brussaard. 2016. "Both Phosphorus-and Nitrogen Limitation Constrain Viral Proliferation in Marine Phytoplankton." *Aquatic Microbial Ecology* 77: 87–97.

Martínez Martínez, J., A. Boere, I. Gilg, et al. 2015. "New Lipid Envelope-Containing Dsdna Virus Isolates Infecting *Micromonas pusilla* Reveal a Separate Phylogenetic Group." *Aquatic Microbial Ecology* 74: 17–28.

Mojica, K. D. A., and C. P. D. Brussaard. 2014. "Factors Affecting Virus Dynamics and Microbial Host–Virus Interactions in Marine Environments." *FEMS Microbiology Ecology* 89: 495–515.

Mojica, K. D. A., J. Huisman, S. W. Wilhelm, and C. P. D. Brussaard. 2016. "Latitudinal Variation in Virus-Induced Mortality of Phytoplankton Across the North Atlantic Ocean." *The ISME Journal* 10: 500–513.

Monier, A., A. Chambouvet, D. S. Milner, et al. 2017. "Host-Derived Viral Transporter Protein for Nitrogen Uptake in Infected Marine Phytoplankton." *Proceedings of the National Academy of Sciences* 114: E7489–E7498.

Nagasaki, K., and M. Yamaguchi. 1998. "Effect of Temperature on the Algicidal Activity and the Stability of HaV (*Heterosigma akashiwo* Virus)." *Aquatic Microbial Ecology* 15: 211–216.

Nanninga, H., and T. Tyrrell. 1996. "Importance of Light for the Formation of Algal Blooms By *Emiliania huxleyi*." *Marine Ecology Progress Series* 136: 195–203.

Nissimov, J. I., J. A. Napier, M. J. Allen, and S. A. Kimmance. 2016. "Intragenus Competition between Coccolithoviruses: An Insight on How a Select Few Can Come to Dominate Many." *Environmental Microbiology* 18: 133–145.

Parada, V., G. J. Herndl, and M. G. Weinbauer. 2006. "Viral Burst Size of Heterotrophic Prokaryotes in Aquatic Systems." *Journal of the Marine Biological Association of the United Kingdom* 86: 613–621.

Ritchie, R. J. 2006. "Consistent Sets of Spectrophotometric Chlorophyll Equations for Acetone, Methanol and Ethanol Solvents." *Photosynthesis Research* 89: 27–41.

Roeber, V. M., I. Bajaj, M. Rohde, T. Schmülling, and A. Cortleven. 2021. "Light Acts as a Stressor and Influences Abiotic and Biotic Stress Responses in Plants." *Plant, Cell & Environment* 44: 645–664.

Selinger, R. L. B., Z.-G. Wang, W. M. Gelbart, and A. Ben-Shaul. 1991. "Statistical-Thermodynamic Approach to Fracture." *Physical Review A* 43: 4396–4400.

Short, S. M., M. A. Staniewski, Y. V. Chaban, A. M. Long, and D. Wang. 2020. "Diversity of Viruses Infecting Eukaryotic Algae." *Current Issues in Molecular Biology* 39: 29–62.

Suttle, C. A. 2005. "Viruses in the Sea." *Nature* 437: 356–361.

Sydney, E. B., A. C. Novak, J. C. de Carvalho, and C. R. Soccol. 2014. "Respirometric Balance and Carbon Fixation of Industrially Important Algae." In Biofuels From Algae, 67–84. Elsevier.

Whitaker, S., P. Geck, M. M. Medveczky, et al. 1995. "A Polycistronic Transcript in Transformed Cells Encodes the Dihydrofolate Reductase of Herpesvirus Saimiri." *Virus Genes* 10: 163–172.

Wilhelm, S., W. Jeffrey, A. Dean, J. Meador, J. Pakulski, and D. Mitchell. 2003. "UV Radiation Induced DNA Damage in Marine Viruses Along a Latitudinal Gradient in the Southeastern Pacific Ocean." *Aquatic Microbial Ecology* 31: 1–8.

Wommack, K. E., and R. R. Colwell. 2000. "Virioplankton: Viruses in Aquatic Ecosystems." *Microbiology and Molecular Biology Reviews* 64: 69–114.

Woodworth, B. D., R. L. Mead, C. N. Nichols, and D. R. J. Kolling. 2015. "Photosynthetic Light Reactions Increase Total Lipid Accumulation in Carbon-Supplemented Batch Cultures of *Chlorella vulgaris*." *Bioresource Technology* 179: 159–164.

Xing, T., K. Gao, and J. Beardall. 2015. "Response of Growth and Photosynthesis of *Emiliania huxleyi* to Visible and UV Irradiances Under Different Light Regimes." *Photochemistry and Photobiology* 91: 343–349.

Yuan, X., K. Yin, P. Harrison, and J. Zhang. 2011. "Phytoplankton Are More Tolerant to UV Than Bacteria and Viruses in the Northern South China Sea." *Aquatic Microbial Ecology* 65: 117–128.

Zhang, R., M. G. Weinbauer, and P. Peduzzi. 2021. "Aquatic Viruses and Climate Change." *Current Issues in Molecular Biology* 41: 357–380.

Zheng, Y., and K. Gao. 2009. "Impacts of Solar Uv Radiation on the Photosynthesis, Growth, and UV-Absorbing Compounds in *Gracilaria lemaneiformis* (Rhodophyta) Grown at Different Nitrate Concentrations." *Journal of Phycology* 45: 314–323.

Supporting Information

Additional supporting information can be found online in the Supporting Information section.